# Study of the Atomic Structure and Phase Separation in Amorphous Si-C-N Ceramics by X-Ray and Neutron Diffraction

S. Schempp, J. Dürr, P. Lamparter, J. Bill, and F. Aldinger Max-Planck-Institut für Metallforschung, Seestraße 92, D-70174 Stuttgart

Z. Naturforsch. 53 a, 127-133 (1998); received February 16, 1998

Amorphous  $Si_{37}C_{32}N_{31}$  and  $Si_{37}C_{29}N_{34}$  ceramics were produced by pyrolysis of a polyhydromethylsilazane precursor. Their structure was investigated by X-ray and neutron diffraction. Wide angle diffraction showed that the Si-atoms are preferentially bonded to nitrogen atoms, but also bonding to carbon atoms was found. This suggests that the excess carbon atoms form an amorphous graphite-like phase. Small angle scattering revealed that the ceramics are inhomogeneous. The evolution of the phase separation during annealing was investigated and it was concluded that amorphous  $Si_3N_4$  precipitates grow in the Si-C-N materials. The results are compared with previous results for amorphous  $Si_{24}C_{43}N_{33}$  produced from a polysilylcarbodiimide precursor [1 - 3].

#### 1. Introduction

Various questions about the structure of precursor derived amorphous Si-C-N ceramics are of importance, such as i) how does the structure depend on the way how it was produced from a polymer, ii) how does the structure change during further heat treatment up to the crystallization process, and iii) how does the structure of an amorphous alloy correlate with its composition, i.e. its location in the ternary Si-C-N phase diagram.

In the present work these questions were addressed during an investigation of the structure of the amorphous ceramics  $Si_{37}C_{32}N_{31}$  and  $Si_{37}C_{29}N_{34}$ , which were obtained by pyrolysis of a commercial polyhydromethylsilazane (*NCP 200*).

The X-ray diffraction diagram of an  $\mathrm{Si}_{37}\mathrm{C}_{32}\mathrm{N}_{31}$  sample in Fig. 1 shows that we have to distinguish between two overlapping scattering regimes: the wide angle scattering regime at  $2\Theta > 5^\circ$ , which contains the information about the atomic short range order, and the small angle scattering regime at  $2\Theta < 5^\circ$ , which is determined by inhomogeneities. The appearance of a strong small angle scattering effect reveals that the amorphous material is not homogeneous. In the present work, both scattering regimes were investigated in order to establish a detailed picture of the structure of amorphous Si-C-N ceramics.

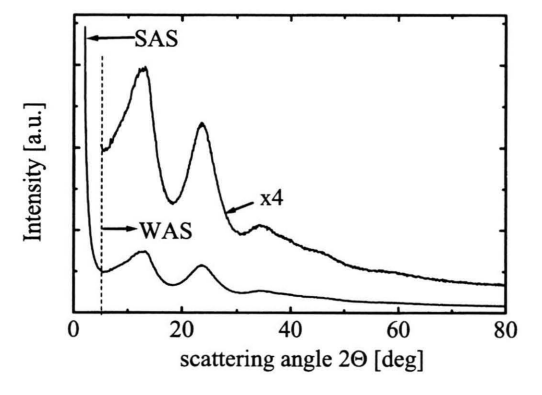


Fig. 1. Amorphous  $Si_{37}C_{32}N_{31}$ : X-ray diffraction diagram showing a small angle (SAS) and a wide angle (WAS) scattering regime. In the WAS regime the curve is plotted also enlarged by a factor of 4.

#### 2. Theoretical Formalism

In the following the essential definitions are briefly summarized. For more details we refer to the review [4].

# 2.1. Atomic Short Range Order and Wide Angle Scattering

From a scattering experiment, after application of the appropriate corrections, the total structure factor S(q) is obtained by normalization of the coherently scattered intensity per atom  $I_{\text{coh}}(q)$  [5]:

$$S(q) = \frac{I_{\text{coh}} - \left[ \langle b^2 \rangle - \langle b \rangle^2 \right]}{\langle b \rangle^2},\tag{1}$$

Reprint requests to Dr. P. Lamparter; Fax: +49 711 2265722.

where  $q = 4\pi(\sin\Theta)/\lambda$  is the wave vector transfer,  $2\Theta$  the scattering angle and  $\lambda$  the wave length. The brackets  $\langle \ \rangle$  denote compositional averages of the scattering lengths  $b_i$  of the atomic species i, with atom fractions  $c_i$ .

The total pair correlation function G(r) is obtained by Fourier transformation of the structure factor

$$G(r) = \frac{2}{\pi} \int_0^\infty q \left[ S(q) - 1 \right] \sin(qr) \, \mathrm{d}q. \tag{2}$$

The total G(r)-function is a weighted sum of the partial pair correlation functions  $G_{ij}(r)$ :

$$G(r) = \sum_{i=1}^{n} \sum_{j=1}^{n} \frac{c_i c_j b_i b_j}{\langle b \rangle^2} G_{ij}(r)$$

$$= \sum_{i=1}^{n} \sum_{j=1}^{n} W_{ij} G_{ij}(r).$$
(3)

In case of a ternary system (n = 3) we need 6 partial  $G_{ij}(r)$ -functions for the structural description of the system (note that  $G_{ij}(r) = G_{ji}(r)$ ).

The partial pair density distribution function

$$\rho_{ij}(r) = c_j \left( \rho_0 + \frac{G_{ij}(r)}{4\pi r} \right), \tag{4}$$

where  $\rho_0$  is the mean atomic number density, describes the number of j-type atoms per unit volume at distance r from an i-type atom at r = 0.

# 2.2. Inhomogeneous Structure and Small Angle Scattering

If the system is not homogeneous, but contains fluctuations of the composition and/or density on a medium range scale beyond the scale of atomic distances, say beyond 10 Å, a small angle scattering effect may be observed [6-8].

In case of the separation of a phase p in a matrix m, the integrated intensity Q, the so called invariant, is

$$Q = \int I(q)q^2 \, dq = 2\pi^2 (\Delta \eta)^2 v(1 - v), \tag{5}$$

where v is the volume fraction of the phase p and  $\Delta \eta = \eta_m - \eta_p$  is the difference of the scattering length densities of p and m.

The mean scattering length density  $\langle \eta \rangle$  of the sample can be calculated from its composition and density:

$$\langle \eta \rangle = \rho_0 \sum_{i=1}^n c_i b_i. \tag{6}$$

On the other side, for a phase separated sample,  $\langle \eta \rangle$  is

$$\langle \eta \rangle = (1 - v)\eta_m + v\eta_p. \tag{7}$$

From (5) and (7) follows

$$v = [1 + 2\pi^{2}(\eta_{p} - \langle \eta \rangle)^{2}/Q]^{-1}.$$
 (8)

## 3. Experimental

### 3.1. Specimen Preparation

The amorphous Si-C-N ceramics were produced by pyrolysis of a polyhydromethylsilazane polymer (NCP 200, Chisso Corporation Japan). Two different routines were employed: The material investigated in the wide angle experiments was directly pyrolyzed at 1050 °C in an argon atmosphere without crosslinking and densification. The heat treatment yielded amorphous Si<sub>37</sub>C<sub>32</sub>N<sub>31</sub> ceramics. The small angle scattering experiments were performed with a batch of samples which have been prepared using the conventional procedures, i. e. crosslinking, ball milling, green body pressing and pyrolysis at 1050 °C as described in [9]. Chemical analysis yielded the composition Si<sub>37</sub>C<sub>29</sub>N<sub>34</sub> and an oxygen contamination of

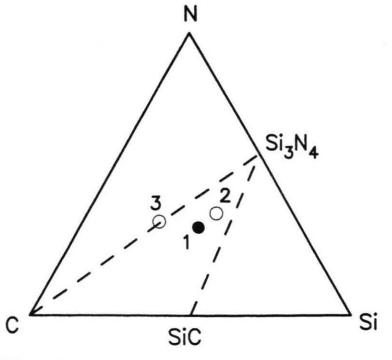


Fig. 2. Si-C-N phase diagram, showing the position of the Si-C-N samples with respect to the quasibinary lines  $Si_3N_4$  - C and  $Si_3N_4$  - SiC. 1:  $Si_{37}C_{32}N_{31}$ , present work, 2:  $Si_{40}C_{24}N_{36}$  [10], 3:  $Si_{24}C_{43}N_{33}$  [1 - 3].

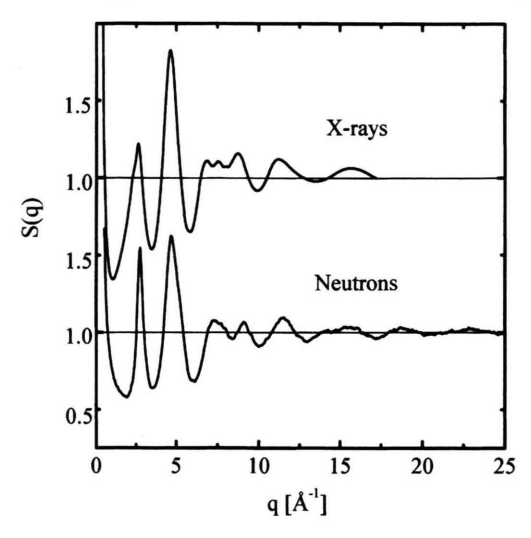


Fig. 3. Amorphous  $Si_{37}C_{32}N_{31}$ : total structure factors from X-ray and neutron diffraction.

about 2 at%. Thus we state that the two different preparation routines yielded almost the same composition. The compositions of the Si-C-N ceramics of the present work and of previous studies are shown in Fig. 2. The density of the ceramics was determined by mercury porosimetry measurements.

#### 3.2. Diffraction Experiments

The X-ray wide angle scattering was measured up to  $q=18~{\rm \AA}^{-1}$  in transmission mode using Ag-K $_{\alpha}$  radiation. The neutron wide angle scattering experiments were performed at the ISIS facility of the Rutherford Appleton Laboratory, UK, using the SANDALS instrument. With this instrument a range of the wave vector transfer up to  $q=25~{\rm \AA}^{-1}$  could be measured with good counting statistics. This extended range of q is essential for the resolution of the individual atomic pairs i-j in r-space. Neutron small angle scattering was done at the BENSC facility of HMI, Berlin, using the V4 instrument.

#### 4. Results and Discussion

### 4.1. Atomic Structure

The total structure factors,  $S_{\rm x}(q)$  from X-ray scattering and  $S_{\rm n}(q)$  from neutron scattering, are shown in Figure 3. The total pair correlation functions  $G_{\rm x}(r)$  and  $G_{\rm n}(r)$ , obtained by Fourier transformation of the

Table 1. Weighting factors  $W_{ij}$  of the partial  $G_{ij}(r)$  according to (3). (x) for X-rays at q = 0, (n) for neutrons.

Sample	$W_{ij}$						
	Si-Si	Si-N	Si-C	N-N	N-C	C-C	
$\overline{Si_{37}C_{32}N_{31}(x)}$	0.312	0.262	0.231	0.055	0.097	0.043	
$Si_{37}C_{32}N_{31}$ (n)	0.055	0.206	0.153	0.193	0.287	0.106	
$Si_{24}C_{43}N_{33}$ (n)	0.021	0.127	0.121	0.193	0.365	0.173	

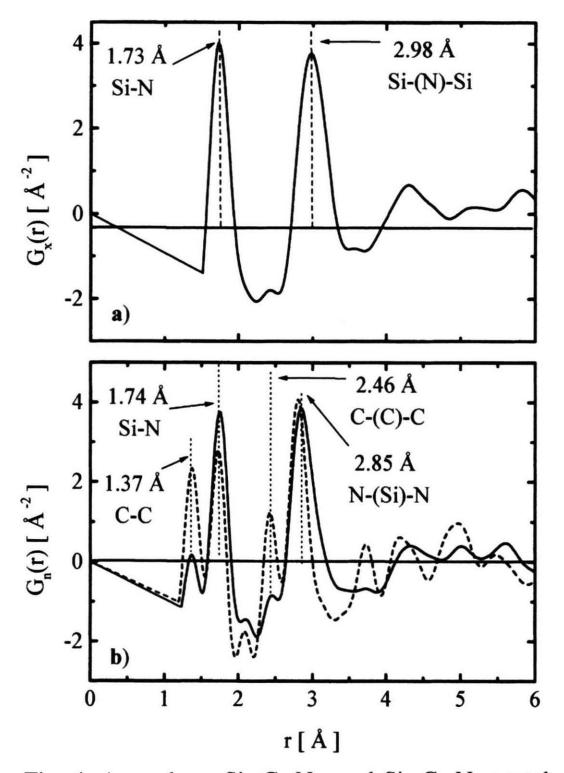


Fig. 4. Amorphous  $Si_{37}C_{32}N_{31}$  and  $Si_{24}C_{43}N_{33}$ : total pair correlation functions, a) from X-ray diffraction, b) from neutron diffraction. The dashed curve is for  $Si_{24}C_{43}N_{33}$  from [1, 3].

structure factors, are shown in Figs. 4 a, b. It is evident that X-ray scattering and neutron scattering yields strongly different runs of the pair correlation functions. With X-rays two distinct peaks, at 1.73 and 2.98 Å, are observed in the range r < 3.5 Å, whereas in the neutron  $G_{\rm n}(r)$  there are four peaks, at 1.37, 1.74, 2.46 and 2.85 Å. On the basis of the atomic sizes of the involved atomic species and the weighting factors  $W_{ij}$  in Table 1 these peaks can be attributed to individual atomic pairs i-j.

In the following discussion the pair correlation functions G(r) of  $Si_{37}C_{32}N_{31}$  will be compared with

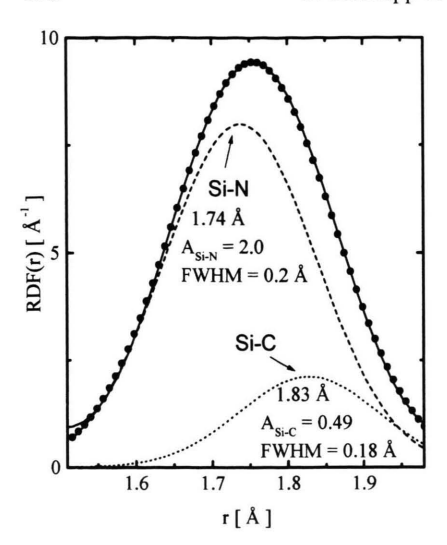


Fig. 5. Amorphous  $Si_{37}C_{32}N_{31}$ : Gaussian fitting with a Si-N and a Si-C contribution to the peak at 1.74 Å of the RDF(r)-function corresponding to  $G_n(r)$  from Fig. 4b. — experimental curve,  $\bullet$  fit.

the  $G_n(r)$  of  $Si_{24}C_{43}N_{33}$  from [1, 3], and also with the related crystalline phases  $Si_3N_4$ [11], SiC [12], graphite [13] and diamond [14].

The peaks at 1.37 and 2.46 Å in the neutron  $G_{\rm n}(r)$  belong to a C-C correlation. With X-rays they are not observed due to the much smaller weighting factor (cf. Table 1). In the study on  ${\rm Si}_{24}{\rm C}_{43}{\rm N}_{33}$  [1, 3], the two peaks were interpreted as due to a separated amorphous graphite-like carbon phase in the ceramics. Note that the peak positions are in good agreement with the distances in graphite at 1.42 and 2.46 Å. Thus it may be concluded that also in the  ${\rm Si}_{37}{\rm C}_{32}{\rm N}_{31}$  ceramics there is an amorphous graphite-like carbon phase. Since the C-C weighting factor for  ${\rm Si}_{37}{\rm C}_{32}{\rm N}_{31}$  is smaller than that for  ${\rm Si}_{24}{\rm C}_{43}{\rm N}_{33}$ , it can be understood that the C-C peaks are less pronounced in the total  $G_{\rm n}(r)$  of  ${\rm Si}_{37}{\rm C}_{32}{\rm N}_{31}$ .

The peak at 1.74 Å reflects the Si-N bonds. Its amplidude is somewhat larger for  $G_{\rm x}(r)$  than for  $G_{\rm n}(r)$  which is in line with the corresponding  $W_{ij}$ . The peak at 2.85 Å in  $G_{\rm n}(r)$  is attributed to an N-N correlation, and the peak at 2.98 Å in  $G_{\rm x}(r)$  to an Si-Si correlation where, however, also underlying contributions from other correlations are supposed. The positions of the latter three peaks are in good agreement with the corresponding distances in crystalline Si<sub>3</sub>N<sub>4</sub>[11] (Si-N at 1.71...1.77 Å, N-N at 2.80...2.94 Å and Si-Si at 2.72...3.15 Å).

The comparison of the two  $G_n(r)$  functions in Fig. 4b shows that the peaks at 1.74 Å (Si-N) and 2.85 Å (N-N) in the  $G_n(r)$  of  $Si_{37}C_{32}N_{31}$  match well at their left flanks with the corresponding peaks at 1.74 and 2.81 Å in the  $G_n(r)$  of  $Si_{24}C_{43}N_{33}$ . However, these peaks are broadened on their right hand sides, compared with the peaks of Si<sub>24</sub>C<sub>43</sub>N<sub>33</sub>, and the peak at 2.85 Å is shifted slightly to a larger rvalue. Since in crystalline SiC a direct Si-C distance appears at 1.89 Å and an indirect C-(Si)-C distance at 3.06 Å, this suggests that in amorphous  $Si_{37}C_{32}N_{31}$ there is also a considerable number of Si-C bonds, which causes the broadening at the right hand side of the peaks at 1.74 and 2.85 Å. Assuming that the peak at 1.74 Å in the G(r) of  $Si_{37}C_{32}N_{31}$  contains two contributions, namely a contribution of a Si-N correlation at about 1.74 Å and a contribution of a Si-C correlation at about 1.89 Å, the corresponding partial average coordination numbers  $Z_{ij}$  can be estimated from the peak areas  $A_{ij}$  using the relation

$$Z_{ij} = \frac{c_j}{c_i} \, Z_{ji} = \frac{c_j}{W_{ij}} \, A_{ij}. \tag{9}$$

The areas  $A_{ij}$  were determined by fitting two Gaussian curves to the peak of the corresponding total radial distribution function

$$RDF(r) = 4\pi r^2 \rho_0 + rG(r),$$
 (10)

as shown in Figure 5. From the Gaussian at 1.74 Å, the average values  $Z_{\rm SiN}=3.0$  and  $Z_{\rm NSi}=3.6$ , and from the Gaussian at 1.83 Å, the values  $Z_{\rm SiC}=1.0$  and  $Z_{\rm CSi}=1.2$  were obtained. The sum  $Z_{\rm Si}=Z_{\rm SiN}+Z_{\rm SiC}=4.0$  proves that the Si-atoms are tetrahedrally coordinated in the amorphous ceramics. It should be noted that we cannot distinguish on the basis of the average values of  $Z_{\rm SiN}$  and  $Z_{\rm SiC}$  between the existence of only  ${\rm SiN_4}$  and  ${\rm SiC_4}$  tetrahedra or the additional existence of C-N mixed tetrahedra  ${\rm Si(C,N)_4}$ . The average number  $Z_{\rm NSi}$  of 3.6 silicon atoms surrounding each nitrogen atom is fairly close to the three-fold coordination of nitrogen in crystalline  ${\rm Si_3N_4}$ .

The wide angle scattering results suggest that within the  $Si_{37}C_{32}N_{31}$  ceramics the nitrogen atoms prefer a three fold silicon coordination in order to form an  $Si_3N_4$ -like structure. The excess silicon bonds are saturated by carbon atoms and the excess carbon forms an amorphous phase of graphite-like carbon. The assumption of non-existing mixed  $Si(C,N)_4$ 

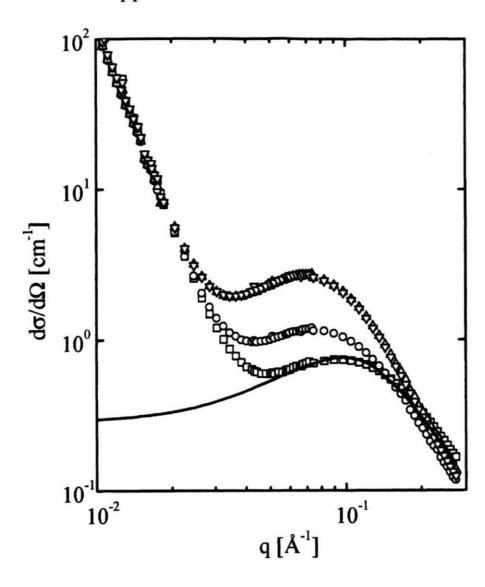


Fig. 6. Amorphous  $Si_{37}C_{29}N_{34}$ : Small angle neutron scattering cross sections after annealing at 1300 °C, ( $\square$ ) 0 h, i. e. only annealed during the heating ramp, ( $\circ$ ) 5 h, ( $\Delta$ ) 10h, ( $\nabla$ ) 15h. ( $\longrightarrow$ ) hard-sphere model.

tetrahedra corresponds to the formal subdivision of the  $Si_{37}C_{32}N_{31}$  ceramics into 54 at%  $Si_3N_4 + 28$  at% SiC + 18 at% C. In the phase diagram of Fig. 2 this ceramics lies in the region between the lines of the two quasi-binary systems  $Si_3N_4 - C$  and  $Si_3N_4 - SiC$ . On the other hand, the  $Si_{24}C_{43}N_{33}$  ceramics, where phase separation into  $Si_3N_4 + C$  and no indication for Si-C bonds was found [1-3], lies on the line of the quasi-binary system  $Si_3N_4 - C$ .

In a previous study on *NCP 200*-derived Si-C-N ceramics [10] it was not possible to obtain information about the environment of the C-atoms. This is probably due to the less extended *q*-range measured in [10], i. e. to lower resolution in real-space.

#### 4.2. Phase Separation

Figure 6 shows the small angle neutron scattering (SANS) cross sections of amorphous  $Si_{37}C_{29}N_{34}$  after annealing at 1300 °C. It is obvious that the material contains inhomogeneities which give rise to the observed SANS signal.

The SANS curves exhibit two regimes which are caused by different phenomena: Towards very small q values the scattered intensities show a linear increase in the log-log plot. This effect is caused by scattering from the surface of pores in the material according to

Table 2. Parameters for different possible amorphous phases segregated in the Si-C-N matrix. D = density,  $\rho_0 =$  number density,  $\eta =$  scattering length density,  $\Delta \eta =$  contrast. <sup>a)</sup> values for the crystalline state were used, <sup>b)</sup> measured with glassy carbon, <sup>c)</sup> measured.

Phase	D [g/cm <sup>3</sup> ]	$\overset{\rho_0}{[\mathring{A}^{-3}]}$	$\eta_{\rm p}$ [10 <sup>10</sup> /cm <sup>2</sup> ]	$(\Delta \eta)^2$ [10 <sup>20</sup> /cm <sup>4</sup> ]
Si <sub>2</sub> N <sub>4</sub>	3.43 <sup>a)</sup>	0.103	7.31	4.84
Si <sub>3</sub> N <sub>4</sub> SiC	3.22a)	0.097	5.24	0.02
C (glassy carbon)	1.53 b)	0.077	5.11	0.00
Si <sub>37</sub> C <sub>29</sub> N <sub>34</sub>	2.39 c)	0.077	5.11	

Porods law [6-8] and was subtracted in the further data evaluation.

At larger q values, a second scattering effect follows which exhibits a peak. This SANS effect depends strongly on the temperature and on the time of annealing. Annealing causes an increase of the intensity and also a shift of the peak towards lower q values, which shows that the size of the scattering regions is growing. The occurrence of a peak indicates an interference effect, which means a substantial volume of distance-correlated regions within the material.

In the following a model for the phase separation of Si<sub>37</sub>C<sub>29</sub>N<sub>34</sub> is proposed which yields a quantitative description of the experimental SANS curves. In Table 2 the relevant parameters of different phases are listed which have to be considered as conceivable scattering regions. The contrast, i. e. the squared difference  $(\Delta \eta)^2$  between the scattering length densities of the regions and the Si-C-N matrix is listed as a measure for the visibility of a certain type of regions in the SANS experiments. It should be noted that the regions, whatever their type, are still amorphous, because wide angle scattering did not indicate any traces of crystalline peaks up to 1400 °C. During crystallization of the Si-C-N ceramics at temperatures above 1400 °C the crystalline phases Si<sub>3</sub>N<sub>4</sub> and SiC occur.

The values for  $(\Delta \eta)^2$  in Table 2 are given for the case of a small volume fraction v of the segregated phase, i. e. for a negligible change of the composition of the Si-C-N matrix. However, in case of a substantial amount of segregated  $\mathrm{Si}_3\mathrm{N}_4$ , the scattering length density of the remaining matrix changes considerably, and thus the contrast between the precipitates and the matrix increases. Figure 7 shows the variation of the contrast  $(\Delta \eta)^2$ , where the change of the matrix with increasing volume fraction v of segregated  $\mathrm{Si}_3\mathrm{N}_4$  is taken into account according to (7). The upper curve

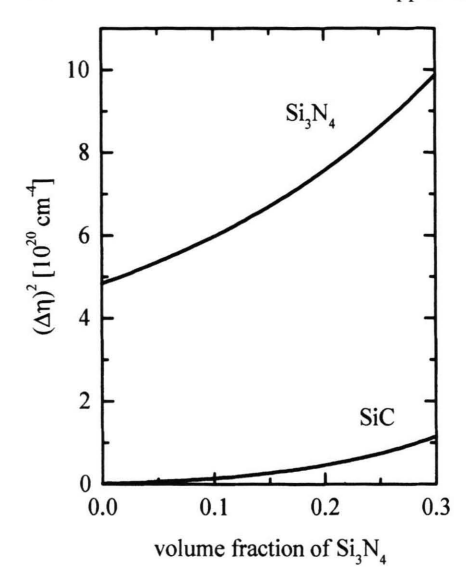


Fig. 7. Amorphous  $Si_{37}C_{29}N_{34}$ : contrast  $(\Delta\eta)^2$  between precipitates,  $Si_3N_4$  or SiC, and Si-C-N matrix versus the volume fraction of the  $Si_3N_4$  precipitates.

shows the contrast between  $\mathrm{Si_3N_4}$  and the changing Si-C-N matrix. The lower curve shows the contrast between SiC precipitates and the Si-C-N matrix which remains after the segregation of an amount v of  $\mathrm{Si_3N_4}$ . We note that the segregation of SiC would not change the scattering length density of the starting matrix because both, SiC and the matrix, have almost the same values of  $\eta$ . In conclusion of this part of the discussion we state that the values of  $\Delta\eta$  in Table 2 and Fig. 7 reveal that the measured SANS effect has to be attributed to an amorphous  $\mathrm{Si_3N_4}$  phase, segregated in the Si-C-N matrix. Segregated SiC or carbon would not yield a contrast sufficient for the measured SANS signals.

The experimental SANS intensities were fitted by a hard-sphere model [6 - 8] for the  $Si_3N_4$ -scattering regions as shown in Fig. 6 for the as-prepared sample:

$$I_{\text{mod}}(q) = S_{\text{cor}}(q) \cdot I_{\text{hs}}(q). \tag{11}$$

 $I_{\rm hs}(q)$  is the scattering from a system of isolated hard spheres, and the structure factor  $S_{\rm cor}(q)$  describes the interference effect due to the positional correlations between the hard spheres. From the fit, the average radius R of the regions and the invariant Q of the scattering were obtained. From the invariant, the volume fraction v of the segregated  ${\rm Si}_3{\rm N}_4$  phase was calculated using (8) which takes into account the change of the matrix composition due to increasing v.

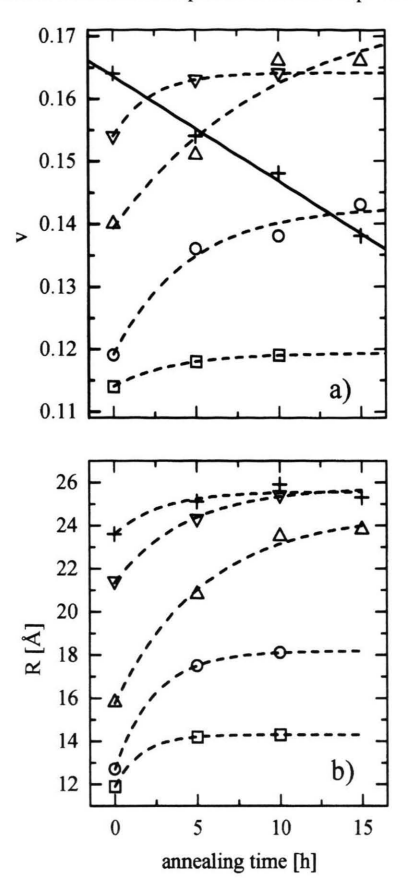


Fig. 8. Amorphous  $Si_{37}C_{29}N_{34}$ : formation of amorphous  $Si_3N_4$  regions during annealing. a) volume fraction, b) radius. ( $\square$ ) 1050 °C, ( $\circ$ ) 1200 °C, ( $\Delta$ ) 1300 °C, ( $\nabla$ ) 1400 °C, (+) 1450 °C. The origin of the time scale refers to the point in the heating curve where the indicated temperature was reached, i. e. it involves the heating ramp.

Figure 8a shows the increase of the volume fraction v of the  $\mathrm{Si}_3\mathrm{N}_4$  phase during the anneals of the ceramics. The dashed lines were fitted using a Gibbs-Evetts-Leake type of annealing function [15]. In the temperature range from 1050 up to 1300 °C the increase is faster at higher temperatures, and at 1400 °C the increase is again less steep. We note that the state of equilibrium, i. e. a saturation of the level of v, is not attained within the time interval of 15 hrs. At 1450 °C the situation changes drastically. We observe a decrease of v, which is explained by the decomposition of the segregated  $\mathrm{Si}_3\mathrm{N}_4$  phase according to  $\mathrm{Si}_3\mathrm{N}_4$  +  $3~\mathrm{C} \rightarrow 3~\mathrm{SiC} + 2~\mathrm{N}_2$  [9].

The temperature-time dependence of the radius R of the scattering regions in Fig. 8b shows an increase from 12 Å in the as-prepared Si-C-N ceramics up

to about 25 Å after a 15 h anneal at 1400 °C. We note that the decrease of v at 1450 °C in Fig. 8a is not associated with a decrease of R. This behaviour is explained by the facts that on the one hand the decomposition affects first the smaller  $\mathrm{Si}_3\mathrm{N}_4$  regions, whereas on the other hand the size R, as established from small angle scattering, is associated mainly with the larger regions.

Concluding the SANS results it should be reminded that the separation of a graphite-like carbon phase in Si-C-N, besides the separation of a Si<sub>3</sub>N<sub>4</sub> phase, as suggested from wide angle scattering, cannot be probed by SANS. This illustrates the importance of a combination of both scattering regimes in an investigation of amorphous ceramics. With future small angle X-ray scattering experiments we expect a contrast between the carbon phase and the Si-C-N matrix.

- [1] J. Dürr, thesis work, University of Stuttgart (1997).
- [2] J. Dürr, S. Schempp, P. Lamparter, J. Bill, S. Steeb, and F. Aldinger, Proc. XIII<sup>th</sup> Int. Conf. on the Reactivity of Solids, Hamburg, Sept. 8-12, 1996, Solid State Ionics 101-103, 1041 (1997).
- [3] J. Dürr, P. Lamparter, J. Bill, S. Steeb, and F. Aldinger, Proc. 7<sup>th</sup> Int. Conf. on the Structure of Non-Crystalline Materials, Sept. 15-19, 1997, Sardegna, Italy, to appear in J. Non-Cryst. Solids (1998).
- [4] P. Lamparter and S. Steeb in: Materials Science and Technology, Vol. 1, Structure of Solids, V. Gerold, edt., VCH, Weinheim 1993, pp. 217-288.
- [5] T. E. Faber and J. M. Ziman, Phil. Mag. 11, 153 (1965).
- [6] A. Guinier and G. Fournet, Small-Angle Scattering of X-Rays, John Wiley & Sons, London Chapman Hall 1955.
- [7] O. Kratky and O. Glatter, Small Angle X-Ray Scattering, Academic Press, London 1982.

#### 5. Conclusions

Amorphous Si-C-N ceramics were produced by pyrolysis of a polyhydromethylsilizane precursor and investigated by X-ray and neutron diffraction. The Siatoms prefer tetrahedral bonding to nitrogen atoms, which leads to an inhomogeneous structure with amorphous  $\mathrm{Si_3N_4}$  precipitates. However, also Si - C bonds exist in the ceramics. The excess C-atoms form graphite-like amorphous carbon.

### Acknowledgements

Thanks are due to the Appleton Laboratory, UK, and the Hahn-Meitner Institute, Berlin, for allocation of beam time. The help of A. Soper and A. Wiedenmann during the neutron diffraction experiments is appreciated.

- [8] L. A. Feigin and D. I. Servgun, Structure Analysis by Small Angle X-Ray and Neutron Scattering, Plenum Press, New York 1987.
- [9] M. Frieß, J. Bill, F. Aldinger, D.V. Szabo, and R. Riedel, Key Engineering Materials 89-91, 95 (1994).
- [10] H. Uhlig, M. Frieß, J. Dürr, R. Bellissent, P. Lamparter, F. Aldinger, and S. Steeb, Z. Naturforsch. 51a, 1179 (1996).
- [11] S. N. Ruddlesden and P. Popper, Acta Cryst. 11, 465 (1958).
- [12] P. T. B. Shaeffer, Acta Cryst. **B 25**, 477 (1969).
- [13] P. Trucano and R. Chen, Nature London 258, 136 (1975).
- [14] T. Hom, W. Kiszenick, and B. Post, J. Appl. Cryst. 8, 457 (1975).
- [15] M. R. J. Gibbs, J. E. Evetts, and J. A. Leake, J. Mat. Sci. 18, 278 (1983).